Palaeogeography, Palaeoclimatology, Palaeoecology 417 (2015) 554–560

Contents lists available at ScienceDirect

Palaeogeography, Palaeoclimatology, Palaeoecology

journal homepage: www.elsevier.com/locate/palaeo

Reconstruction of drought variability in North China and its association with sea surface temperature in the joining area of Asia and Indian–Pacific Ocean

Qiufang Cai [a,*], Yu Liu [a,b], Han Liu [a,c], Junli Ren [a,c]

[a] State Key Laboratory of Loess and Quaternary Geology, Institute of Earth Environment, Chinese Academy of Sciences, Xi'an 710075, China
[b] Department of Environmental Science and Technology, School of Human Settlements and Civil Engineering, Xi'an Jiaotong University, Xi'an 710049, China
[c] University of Chinese Academy of Sciences, Beijing, China

ARTICLE INFO

Article history:
Received 10 June 2014
Received in revised form 3 October 2014
Accepted 15 October 2014
Available online 22 October 2014

Keywords:
Tree-ring width
North China
Drought reconstruction
Indian–Pacific Ocean SST
East Asian summer monsoon

ABSTRACT

Using tree-ring data from the northernmost marginal area of the East Asian summer monsoon (EASM) in North China, May–July mean Palmer drought severity index (PDSI) was reconstructed back to 1767 AD. The reconstruction captured 52.8% of the variance over the calibration period from 1945 to 2005 AD and showed pronounced pluvial periods during 1850–1905, 1803–1811 and 1940–1961 and dry periods during 1814–1844, 1916–1932 and 1984–2012. These anomalous periods have previously been reported in other parts of North China. Spatial correlation analyses and comparisons with other hydroclimatic indices in North China indicated that our new PDSI reconstruction could represent spatial and temporal drought variability in this region well. Our work also suggested that the drying tendency currently observed in the northern part of North China (including the study area) is consistent with the weakening of the EASM. Meanwhile the drying trend was seemingly restrained at present in the southern part of North China. Spatial correlation patterns with global sea surface temperature (SST) indicated that the regional hydroclimatic variability in North China was tightly linked to SST over the joining area of Asia and Indian–Pacific Ocean (AIPO), especially over the tropical western Pacific. When SST from prior November to current July (NJ-SST) in the AIPO area was anomalously high (low), the thermal contrast between Asian land and ocean was weakened (strengthened), and the EASM was correspondingly weakened (strengthened), thereby causing droughts (pluvials) in North China. The results of this study do not only provide useful information for assessing the long-term climate change in North China, but also suggest that abnormal variability in NJ-SST over the AIPO area could be used to forecast hydroclimatic conditions in North China.

1. Introduction

The negative impacts of extreme climatic events are usually more obvious in ecologically fragile regions, such as arid to semi-arid areas of the world. North China, one of the main industrial and agricultural (mainly wheat and maize) production areas in China, is facing severe problems of water shortage (Fu and Ma, 2008). Frequently occurring droughts in this area are mainly attributed to a decrease in precipitation (Ma, 2007; Z.X. Hao et al., 2010; Qian et al., 2011; Cai et al., 2014). In addition, recent warming can increase water shortages in this region by exacerbating surface evapotranspiration (Ma and Fu, 2003, 2006). Many previous studies have analyzed the characteristics and possible reasons of drought in North China. The summer droughts of recent decades in this region were generally considered to be related to variability in the East Asian summer monsoon (EASM) (Qian et al., 2012), variation in the Pacific Decadal Oscillation (PDO) (Qian and Zhou, 2014), atmospheric circulation anomalies in the northern hemisphere (L.S. Hao et al., 2010), as well as unreasonable human activity (Fu and Wen, 2002). Special attention was also given to understand the relationship between drought in North China and tropical sea surface temperature (SST) and air–sea interaction (Wu et al., 2001, 2006; Dong et al., 2013). However, these studies were mainly based on a limited data length, not enough to capture the full range of climate variability. Is North China currently experiencing an anomalous drought? What are the long-term physical mechanisms driving drought variability in North China? These questions are still under debate. To answer them, long-term drought indices considering both precipitation and temperature are needed to put current changes in a longer-term perspective.

There are several drought indices using both precipitation and temperature, such as the Reconnaissance Drought Index (RDI) (Tigkas et al., 2013), Walter climate index (Breckle, 2002), Integrated Surface Drought Index (ISDI) (Wu et al., 2013) and Palmer drought severity index (PDSI). PDSI is based on a supply-and-demand model of soil moisture, which considers both the cumulative effect of precipitation and temperature change (Palmer, 1965). It is the most widely used drought

* Corresponding author. Tel.: +86 29 88321726; fax: +86 29 88320456.
E-mail address: caiqf@ieecas.cn (Q. Cai).

http://dx.doi.org/10.1016/j.palaeo.2014.10.021
0031-0182/

index and has proven most effective in determining long-term drought lasting over years, decades and more (Cook et al., 2010). Monthly PDSI is now available over global land areas on a 2.5° × 2.5° grid (Dai et al., 2004). Tree rings are a high-resolution climatic proxy source, which is powerful for reflecting drought variation in monsoon Asia (Liang et al., 2007; Wang et al., 2008; Cook et al., 2010; Fang et al., 2013; Yang et al., 2014). To date, several tree-ring hydroclimatic investigations have been carried out in the south-central part of North China (Li et al., 2006; Sun et al., 2012; Cai and Liu, 2013; Cai et al., 2014). However, existing dendroclimatic research is not enough to fully reveal the characteristics of hydroclimatic variation in North China and the mechanisms responsible for this variation. The goal of this work was to examine the evolution of drought variability in North China through a >240-year PDSI reconstruction derived from absolutely dated and annually resolved tree-ring data. The temporal and spatial representativeness were subsequently investigated, and the possible driving forces of the drought variation in North China were analyzed.

2. Material and methods

2.1. Study area and tree-ring materials

Tree-ring cores were collected from Chinese pine (*Pinus tabuliformis* Carr.) in two different sites located in the northern part of North China (Fig. 1). The first site is the Hengshan Mountain (HSM) (113°43′47″ E, 39°40′ N, 1710–1780 m a.s.l.), where 66 cores from 33 healthy Chinese pine trees were sampled at breast height in August, 2009. The other site is in the Xiaowutai Mountain (LHS) (114°41.22′ E, 39°45.22′ N, 1567 m a.s.l.), where 50 cores from 28 living trees were collected in July 2013. The distance between the two sampling sites is about 80 km. In both sites, Chinese pine is the dominant species. The trees here are growing on a rocky substrate with shallow soil layers. The tree canopies are rather open at these sites.

The study sites are located at the northern edge of the EASM (Tang et al., 2010). Thus, climate in this region is strongly influenced by EASM variation. It is characterized by large precipitation variability, both on annual and interannual scales. Based on the meteorological data from the two nearby meteorological stations Datong (113°20′ E, 40°06′ N, 1067.2 m a.s.l., 1955–2012) and Yuxian (114°34′ E, 39°50 ′N, 909.5 m a.s.l., 1954–2012) (Fig. 1), the annual mean temperature ranges from 6.9 °C in HSM to 8.5 °C in LHS and the mean total precipitation ranges from 377.1 mm to 408.7 mm, respectively. The monthly distributions of precipitation, temperature and relative humidity of the study area are shown in Fig. 2.

Back in the laboratory the tree-ring samples were mounted on wooden core mounts and polished with gradually finer sand paper until the tree-ring boundaries were clear, according to standard dendrochronological techniques (Stokes and Smiley, 1996). Crossdating was done using the traditional skeleton plot method to assign calendar years to each growth ring before tree rings in each core were measured to the nearest 0.01 mm. The LINTAB measuring device connected with a binocular microscope and TSAP software (Rinn, 1996) was used to measure tree-ring width. The COFECHA program (Holmes, 1983) was then utilized to evaluate the quality of crossdating and ring-width measurements. Young trees and tree-ring series with anomalous growth patterns and poor correlations with the majority of the other samples were omitted from further analyses.

In this study, we standardized ring-width series using the program ARSTAN (Cook and Kairiukstis, 1990). First we fit a negative exponential curve or straight line with negative slope to each raw ring-width measurement series, and then divided the actual ring widths by the corresponding fitted curve value. The resulting dimensionless indices were then combined to produce a single STD chronology by means of "biweight robust mean". The reliable starting year of the chronology was assessed using the subsample signal strength (SSS) threshold value of 0.85 (Wigley et al., 1984) because the early years did not have enough sample replication.

2.2. Climate data

Monthly meteorological records from Datong and Yuxian stations were averaged together to produce regional composite meteorological series from 1955 to 2012 (Fig. 2). Monthly mean temperature, relative humidity and monthly total precipitation records from previous October to current September were chosen as target variables for further analysis. Moreover, considering that the sampling sites belong to a semi-arid area, where tree growth may be limited by moisture conditions, PDSI from the nearest grid point (38.75° N, 113.75° E) covering the 1945 to 2005 time-span (Dai et al., 2004), was extracted for this study (henceforth referred to as Dai-PDSI).

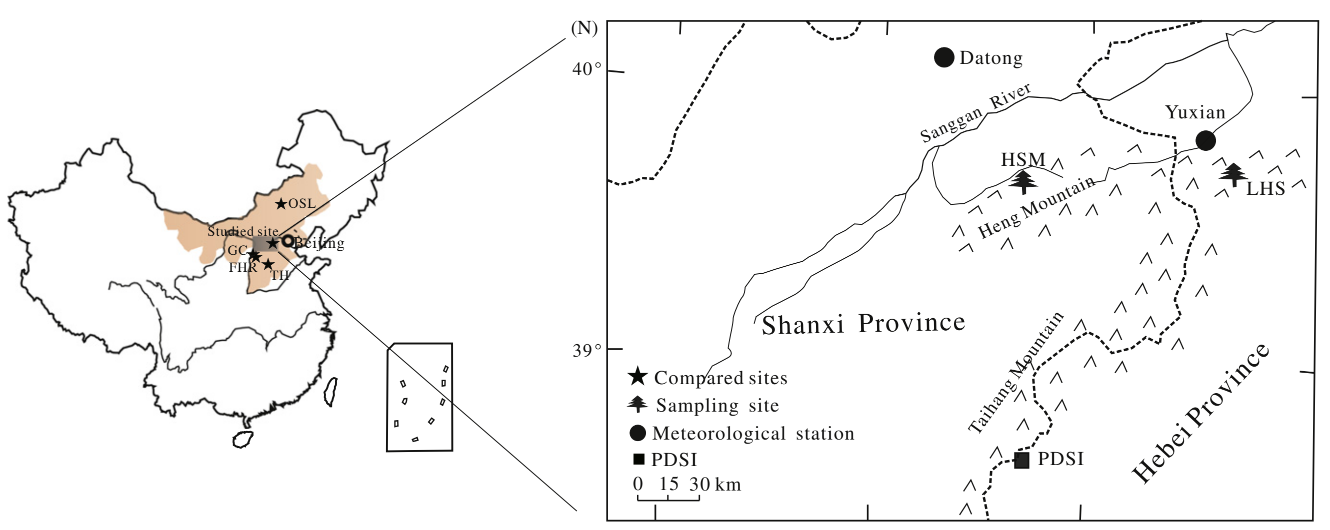

Fig. 1. Map showing the location of the two sampling sites, two meteorological stations and the PDSI grid point. The current PDSI reconstruction was compared to existing reconstructions from Guancen Mountian (GC), Fenhe River (FHR), Taihang Mountian (TH) and Ortindag Sand Land (OSL). The area highlighted in orange indicates the general location of North China.